Korean J Physiol Pharmacol 2024;28(4):313-322
https://doi.org/10.4196/kjpp.2024.28.4.313

KJPP

Original Article

Requirement of β subunit for the reduced voltage-gated Na^+ current of a Brugada syndrome patient having novel double missense mutation (p.A385T/R504T) of *SCN5A*

Na Kyeong Park[1,#], Seong Woo Choi[2,3,#], Soon-Jung Park[4,#], JooHan Woo[2,3], Hyun Jong Kim[2,3], Woo Kyung Kim[3,5], Sung-Hwan Moon[6,*], Hun-Jun Park[7,*], and Sung Joon Kim[1,8,*]

[1]*Department of Physiology, Seoul National University College of Medicine, Seoul 03080,* [2]*Department of Physiology, Dongguk University College of Medicine, Gyeongju 38066,* [3]*Channelopathy Research Center (CRC), Dongguk University College of Medicine, Goyang 10326,* [4]*R&D Center, Biosolvix Co. Ltd, Seoul 08502,* [5]*Department of Internal Medicine Graduate School of Medicine, Dongguk University, Goyang 10326,* [6]*Department of Animal Science and Technology, Chung-Ang University, Anseong 17546,* [7]*Division of Cardiology, Department of Internal Medicine, Uijeonbu St.Mary's Hospital, The Catholic University of Korea, Seoul 11765,* [8]*Department of Physiology & Ischemic/Hypoxic Disease Institute, Seoul National University College of Medicine, Seoul 03080, Korea*

ARTICLE INFO

Received March 25, 2024
Revised April 2, 2024
Accepted April 2, 2024

***Correspondence**
Sung-Hwan Moon
E-mail: moonsh@cau.ac.kr
Hun-Jun Park
E-mail: cardioman@catholic.ac.kr
Sung Joon Kim
E-mail: sjoonkim@snu.ac.kr

Key Words
Cardiac arrhythmia
Brugada syndrome
Missense mutation
NAV1.5 voltage-gated sodium channel
Sodium channel beta subunit

#These authors contributed equally to this work.

ABSTRACT Mutations within the *SCN5A* gene, which encodes the α-subunit 5 ($Na_V1.5$) of the voltage-gated Na^+ channel, have been linked to three distinct cardiac arrhythmia disorders: long QT syndrome type 3, Brugada syndrome (BrS), and cardiac conduction disorder. In this study, we have identified novel missense mutations (p.A385T/R504T) within *SCN5A* in a patient exhibiting overlap arrhythmia phenotypes. This study aims to elucidate the functional consequences of *SCN5A* mutants (p.A385T/R504T) to understand the clinical phenotypes. Whole-cell patch-clamp technique was used to analyze the $Na_V1.5$ current (I_{Na}) in HEK293 cells transfected with the wild-type and mutant *SCN5A* with or without *SCN1B* co-expression. The amplitude of I_{Na} was not altered in mutant *SCN5A* (p.A385T/R504T) alone. Furthermore, a rightward shift of the voltage-dependent inactivation and faster recovery from inactivation was observed, suggesting a gain-of-function state. Intriguingly, the co-expression of *SCN1B* with p.A385T/R504T revealed significant reduction of I_{Na} and slower recovery from inactivation, consistent with the loss-of-function in Na^+ channels. The *SCN1B* dependent reduction of I_{Na} was also observed in a single mutation p.R504T, but p.A385T co-expressed with *SCN1B* showed no reduction. In contrast, the slower recovery from inactivation with *SCN1B* was observed in A385T while not in R504T. The expression of *SCN1B* is indispensable for the electrophysiological phenotype of BrS with the novel double mutations; p.A385T and p.R504T contributed to the slower recovery from inactivation and reduced current density of $Na_V1.5$, respectively.

INTRODUCTION

The genetic landscape underlying cardiac arrhythmia disorders has seen remarkable progress in recent years, with a growing understanding of the intricate interplay between ion channels and their role in maintaining normal cardiac rhythm [1]. *SCN5A* is a critical gene in electrical signaling, encoding the alpha subunit of the voltage-gated sodium channel ($Na_V1.5$), which facilitates sodium ion influx into cardiomyocytes during depolarization, a key process in generating cardiac action potentials and conduc-

This is an Open Access article distributed under the terms of the Creative Commons Attribution Non-Commercial License, which permits unrestricted non-commercial use, distribution, and reproduction in any medium, provided the original work is properly cited.
Copyright © Korean J Physiol Pharmacol, pISSN 1226-4512, eISSN 2093-3827

Author contributions: N.K.P., S.W.C., and S.J.P. performed the experiments and analyzed data. H.J.K., J.H.W., and W.K.K. discussed the results and commented on the manuscript. S.H.M., H.J.P., and S.J.K. supervised and coordinated the study. N.K.P., S.W.C., and S.J.K. wrote the manuscript.

tion [2]. Mutations in *SCN5A* can lead to functional impairments of the $Na_V1.5$, potentially resulting in aberrant cardiac electrical activity and an elevated risk of arrhythmogenic events [3]. Such genetic alterations are associated with a spectrum of cardiac arrhythmias, including congenital long QT syndrome (LQTS), Brugada syndrome (BrS), cardiac conduction disorder, dilated cardiomyopathy, and multifocal ectopic Purkinje-related premature contractions [3-5]. Notably, *SCN5A* mutations associated with BrS leads to decreased sodium channel activity due to reduced $Na_V1.5$ protein levels, malfunctioning channel expression, or alterations in gating characteristics such as delayed activation and premature inactivation [2].

Initially, different *SCN5A*-related disorders were regarded as distinct clinical conditions, characterized by unique and isolated symptoms resulting from specific biophysical alterations caused by *SCN5A* mutations on the $Na_V1.5$. However, numerous studies have revealed cases of individuals carrying *SCN5A* variants that do not align with these conventional disorders [6,7]. Instead, these individuals exhibited overlap syndromes, which combine aspects of different canonical *SCN5A*-related arrhythmia syndromes, or they displayed a variable arrhythmic phenotype among individuals with the same mutation [7]. The concept of *SCN5A* overlap syndromes has evolved since its first description in 1999 when an *SCN5A*-1795insD mutation was identified [8]. Various *SCN5A* mutations have since been associated with a wide range of clinical phenotypes, including LQT3, BrS, conduction disorders, sinus nodal dysfunction, atrial standstill, and more [9]. The p.1795insD, p.L1786Q, and p.E1784K mutations in the *SCN5A* gene are linked to a combined phenotype of LQT3 and BrS, characterized by reduced peak Na^+ currents and induction of late Na^+ currents [10].

These electrophysiological alterations contribute to QT interval prolongation and ST elevation on electrocardiogram (ECG), indicative of the overlap in LQT3 and BrS phenotypes. Nevertheless, the underlying mechanisms linking ion channel function and this clinical phenotype are not yet fully understood due to the complexity of overlap syndrome. Electrophysiological studies on mutant *SCN5A* are required to understand the biophysical alterations of ion channels that affect clinical phenotypes.

Here we report a functional study of a $Na_V1.5$ channel involving the novel double missense mutations of p.A385T/R504T in *SCN5A* in a patient showing an abnormal ECG consistent with QRS complex widening, a coved type elevated ST-segment in V2, and QTc prolongation. The p.A385T and p.R504T are situated in the loop connecting transmembrane segments 5 to 6 in domain 1 (S5-S6 in DI) and segments 6 to 1 between domain 1 and 2 (DI-DII linker), respectively (NM_000335.5). In a previous report, Chae *et al.* [11] classified the p.A385T/R504T mutation as a cause of LQT3, but without electrophysiological investigation. To elucidate the pathophysiological association of the mutation with overlap phenotypes, we investigated electrophysiological analysis of the double mutations, including the individual contribution of p.A385T and p.R504T.

METHODS

Clinical data

Clinical data from a patient exhibiting an overlap syndrome of BrS and intraventricular conduction delay were used in this study. The patient underwent clinical evaluation, including an ECG, at Seoul St. Mary's Hospital in Seoul, Korea. Informed consent was obtained from the patient.

DNA constructs, mutagenesis, HEK cell culture and transfection

A human embryonic kidney cell line (HEK293 cell) was cultured in Dulbecco's Modification of Eagle's Medium (Gibco Life Technologies) containing 10% fetal bovine serum and 1% antibiotic-antimycotic solution at 37°C with 5% CO_2. A pCMV6-XL4 vector subcloned *SCN5A* cDNA, double mutants p.A385T(c.1153G>A)/R504T(c.1511G>C), p.A385T, and p.R504T (NM_000335.5) were generated by site-directed mutagenesis. *SCN1B* plasmid originates from Origene (RC209565) and co-transfected with the same amounts of *SCN5A*. Lipofectamine 3000 (Thermo-Fisher, L30000001) transfection reagent was used for electrophysiology analysis to transiently introduce 1 μg of constructs into HEK293 cells according to the manufacturer's instructions. Samples were visualized using a confocal microscope (LSM-700; Carl Zeiss) at the Cardiovascular and Metabolic Research Core Support Center at Inje University, South Korea. Co-transfection of a green fluorescent protein (GFP) ensured successful transfection, and only enhanced green fluorescent protein (EGFP)-positive cells were used for patch clamp analysis at least 24 h post-transfection.

Electrophysiology

All whole-cell Na^+ currents were recorded at room temperature using the standard whole cell patch-clamp technique. The pipette solution contained 20 mM NaCl, 115 mM CsCl, 1 mM $MgCl_2$, 5 mM HEPES, 5 mM EGTA, 0.4 mM NaGTP, and 4 mM MgATP (pH adjusted to 7.2 with CsOH); the bath solution contained 130 mM NaCl, 4 mM CsCl, 10 mM glucose, 10 mM HEPES, 2 mM $CaCl_2$, 1 mM $MgCl_2$ (pH 7.4 with NaOH). The currents were amplified and filtered using an Axopatch 200B amplifier and subsequently digitized at 5 kHz using Digidata 1550B (Molecular Devices) after analog filtering with 20 kHz of the amplifier. In most of our experimental conditions, the general access resistance ranged from 2 to 4 MΩ. To minimize voltage-clamp error, we compensated for the series resistance electronically by 80%. The data were acquired using pClamp 11.1 (Molecular Devices) and analyzed using Clampfit 11.1 (Molecular Devices). Voltage-clamp protocols are provided as insets within each figure.

Western blot

For Western blot analysis, the expression vector pEGFP-N1 was used to subclone WT-*SCN5A* and A385T/R504T-*SCN5A* upstream of the coding region of a GFP. Western blot was performed using whole cell lysates from HEK293 cells that heterologously expressed wild type (WT), and A385T/R504T with β1-subunit *SCN1B*. The cells were lysated with a lysis buffer comprising 150 mM NaCl, 50 mM Tris-Cl (pH 7.4), 1 mM EDTA, and 1% Triton-X 100, and the protein concentration was determined using a BCA Protein Assay Kit (Thermo-Fisher, 23227). Next, 5X SDS-PAGE loading buffer (Biosesang, S2002) was added to the lysates, which were then separated on 8% SDS-PAGE gels and transferred to PVDF membranes. The membranes were incubated with primary antibodies, including a rabbit anti-GFP (1:1,000, Invitrogen, A-11122), and mouse anti-Na-K ATPase (1:2,000, Sigma, 05-369) overnight at 4°C, followed by a secondary antibody (1:10,000) for 1 h at room temperature. Chemiluminescence was used to detect the membrane signals, and protein expression levels were normalized to anti Na-K ATPase and quantified using ImageJ (National Institutes of Health).

Statistical analysis

The results are expressed as mean ± standard error of mean, and statistical comparisons were made by Student t-test using GraphPad prism 8, with $p < 0.05$ indicating significance. Multi-exponential functions were fitted to the data using the nonlinear least-squares method with Origin software.

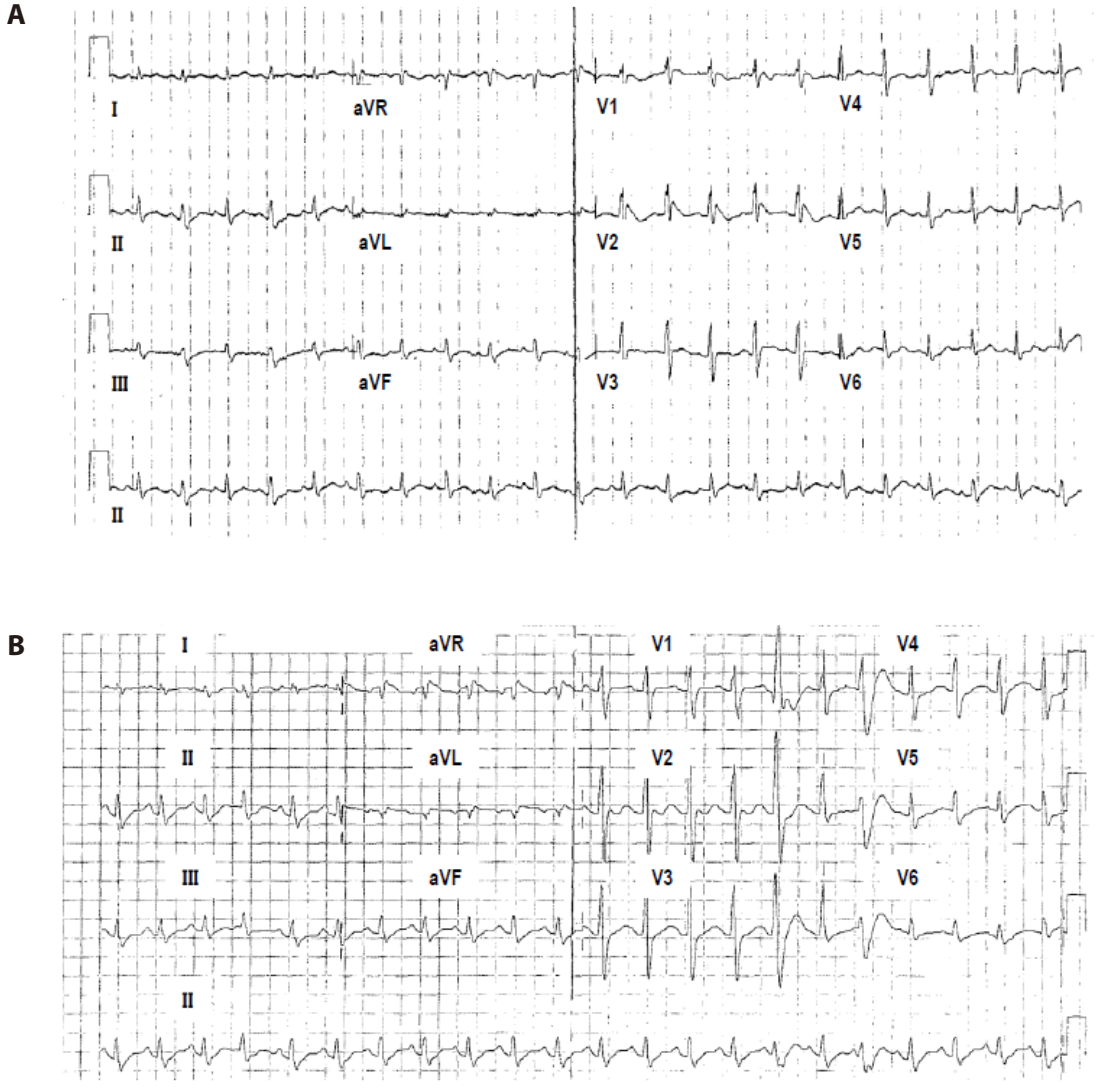

Fig. 1. Twelve-lead electrocardiogram (ECG) of a patient with overlap syndrome with a double missense mutation in *SCN5A*. (A) Representative ECG showed a coved type ST-segment elevation in leads V2 (2 mm) and T-wave abnormality. (B) Representative ECG showed intraventricular conduction delay with prolonged QRS widening to 121 ms (normal value < 100 ms).

RESULTS

SCN5A double mutation case in a patient with overlap syndrome of BrS and intraventricular conduction delay

Here, we reported a case showing overlap syndrome with double mutation in *SCN5A*. After resuscitation from sudden cardiac arrest caused by ventricular fibrillation, a patient showed coved-type elevated ST-segment in leads V2 (2 mm) which meets the ECG criteria for BrS (Fig. 1A, heart rate 132 bpm, QRS duration 100 ms, QT/QTc 300/444 ms), along with the widening of QRS duration to 121 ms (normal value < 100 ms) in ECG examination (Fig. 1B, heart rate 128 bpm, QRS duration 121 ms, QT/QTc 246/359 ms).

Indistinguishable I_{Na} properties of A385T/R504T with *SCN5A* alone

To find the electrophysiological properties caused by this dou-

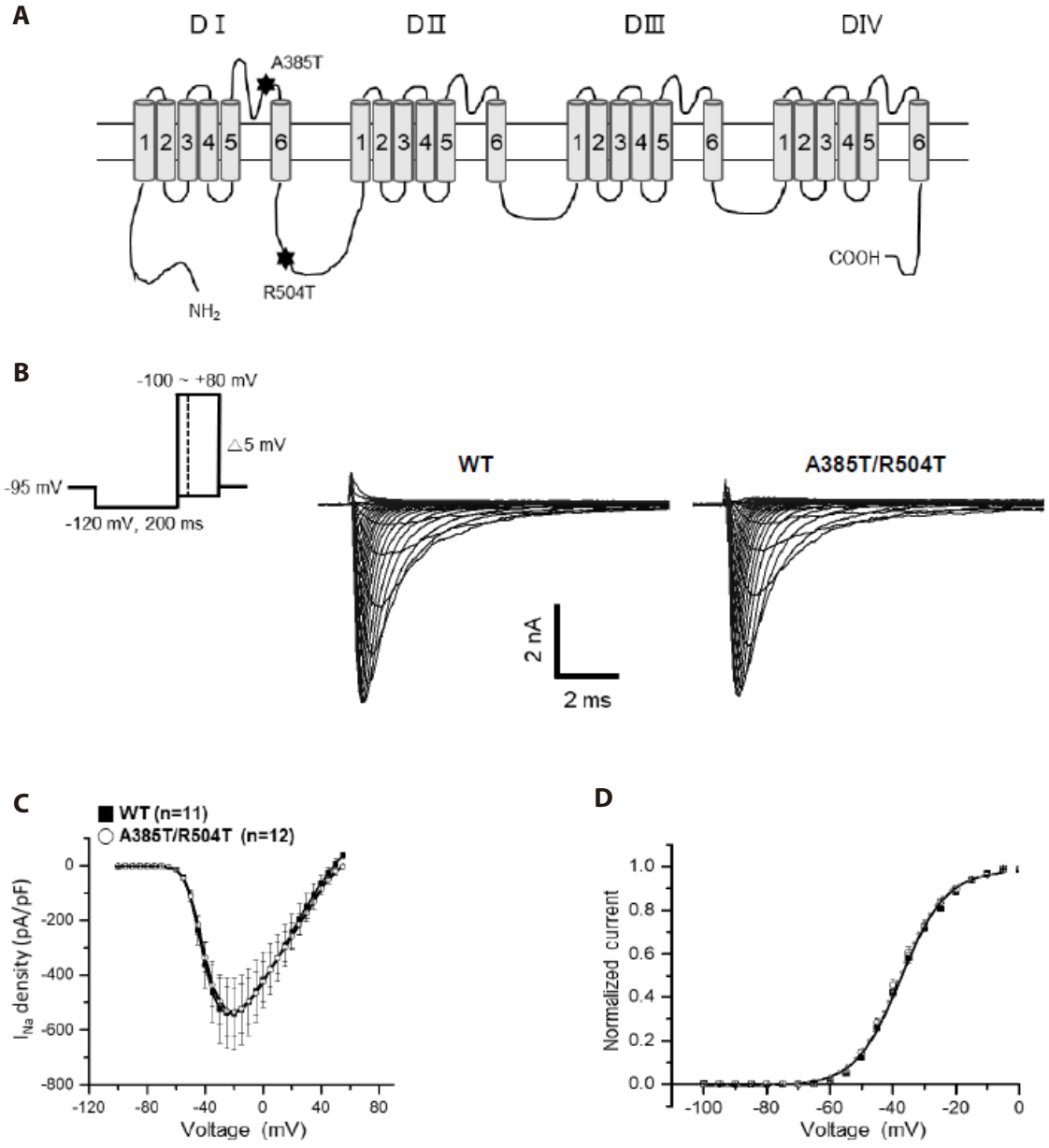

Fig. 2. p.A385T/R504T does not affect Na^+ current (I_{Na}) density. (A) Schematic drawing of the cardiac voltage-gated Na^+ channel α-subunit ($Na_V1.5$) showing position of the A385T/R504T in the loop connecting transmembrane segments 5 and 6 in domain 1 (S5-S6 in DI) and segments 6 and 1 between domain 1 and 2 (DI-DII linker). (B) Representative whole-cell Na^+ current recordings of WT and p.A385T/R504T. (C) Average Na^+ current-voltage (I-V) relation for WT and p.A385T/R504T channels. (D) Voltage-dependence of activation for WT and p.A385T/R504T channels by normalizing peak conductance against the membrane voltage. WT, wild type.

ble mutation, whole cell patch clamp experiment was conducted and compared between WT and double mutant *SCN5A* (p.A385T/R504T) overexpressed HEK293 cells. Step-like depolarizing pulses were applied to activate I_{Na} (Fig. 2B, inset). As shown by the average current-voltage (I-V) relations, the peak amplitude of I_{Na} density was not different between WT and A385T/R504T (WT: maximum I_{Na} –542.21 ± 130.21 pA/pF, n = 11; A385T/R504T: maximum I_{Na} –534.46 ± 90.23 pA/pF, n = 12) (Fig. 2C). The I-V curves were converted to the conductance-voltage (G-V) curve in order to analyze the voltage dependence of activation of $Na_V1.5$ (Fig. 2D), which was not different between WT and p.A385T/R504T (Table 1).

To assess the voltage dependency of inactivation, a two-pulse protocol was employed; 500 ms conditioning pre-pulses ranging from –140 to –15 mV to induce steady-state inactivation, followed by a 50 ms test pulse (Fig. 3A, inset). The voltage dependent of inactivation in p.A385T/R504T was shifted to the rightward direction by 5.73 mV (Table 1), implying increased 'window current' (Fig. 3B).

To measure the recovery from inactivation of $Na_V1.5$, another type of two-pulse protocol with incremental increase of the pulse interval was applied (Fig. 3C). This protocol involved the conditioning pre-pulse (P1; –20 mV, 100 ms) to inactivate $Na_V1.5$, followed by variable hyperpolarized interval (recovery period; –120 mV, 1–1,000 ms) and the second test pulse (P2; –20 mV, 20 ms) (Fig. 3D, inset). The peak amplitudes in response to the P2 were normalized to the peak amplitudes at P1, and the resulting curve was plotted against the inter-pulse recovery period (Fig. 3D). When the curve was fit to a double exponential function, the fast- and slow-time constants of recovery from inactivation showed no difference between WT and p.A385T/R504T (Fig. 3D, right panel bar graphs).

Disclosure of loss-of-function phenotype with *SCN1B* co-expression

When the β1 subunit of $Na_V1.5$ (*SCN1B*) was co-expressed in HEK293 cell, the density of I_{Na} was markedly reduced in p.A385T/R504T (WT + β1: I_{peak} –451.31 ± 77.49 pA/pF (n = 12); p.A385T/R504T + β1: I_{peak} –234.85 ± 28.44 pA/pF (n = 28), Fig. 4A–C), without affecting the voltage dependence of activation (Fig. 4D, Table 1). The immunoblotting analysis showed that the total protein expression of *SCN5A* was not reduced regardless of the *SCN1B* expression. However, a significant decrease in surface protein expression was observed upon co-expression with *SCN1B* (Fig. 4E, $p < 0.05$). Also, the voltage dependence of inactivation was not different between WT and p.A385T/R504T when co-expressed with *SCN1B* (Fig. 5A, B, Table 1). Interestingly, the fast component of recovery from inactivation was slower in p.A385T/R504T with *SCN1B* (Fig. 5C, D).

Different contribution of A385T and R504T in the presence of *SCN1B*

To elucidate the contribution of individual missense mutation of p.A385T/R504T, site-directed mutants of p.A385T and p.R504T were exclusively induced in *SCN5A* and co-expressed with *SCN1B*. The p.R504T + β1, but not p.A385T + β1, resulted in considerably decreased I_{Na} density when compared WT (WT + β1: I_{peak} –451.31 ± 77.49 pA/pF, n = 12; A385T + β1: I_{peak} –430.08 ± 68.76 pA/pF, n = 19; A385T + β1: I_{peak} –239.73 ± 43.31 pA/pF, n = 13) (Fig. 6A, B). The voltage dependence of activation and inactivation remained unchanged in each mutant (Fig. 6C, Table 1). Interestingly, the recovery from inactivation was significantly slower in p.A385T + β1 while not in p.R504T + β1 (fast time constant; p = 0.0001, slow time constant; p = 0.0046, Fig. 6D).

DISCUSSION

Here we investigated the electrophysiological characteristics of the *SCN5A* mutant p.A384T/R504T in an overlap syndrome patient presenting QRS widening and spontaneous ST-segment elevation. The density of I_{Na} was unchanged with p.A385T/R504T alone, but a rightward shift in voltage-dependent of inactivation and faster recovery from inactivation indicated a gain-of-function, contrary to the BrS phenotype. Co-expression with β1 and p.A385T/R504T resulted in reduced I_{Na} and slowed recovery, consistent with BrS. Total *SCN5A* protein expression remained constant in p.A385T/R504T, but membrane protein decreased when co-expressed with β1. Both p.A385T and p.R504T showed characteristic β1-dependent biophysical loss of function, with

Table 1. Voltage- and time-dependence of activation and inactivation for WT and mutant channels

	WT	p.A385T	p.R504T	p.A385T/R504T	WT + β1	p.A385T + β1	p.R504T + β1	p.A385T/R504T + β1
Activation	(n = 12)	(n = 12)	(n = 11)	(n = 12)	(n = 19)	(n = 16)	(n = 12)	(n = 7)
$V_{1/2}$ (mV)	–37.48	–35.36	–37.33	–38.44	–34.09	–32.77	–34.03	–34.45
k (mV)	7.15	7.14	7.15	7.14	7.76	7.73	7.54	7.68
Inactivation	(n = 16)	(n = 15)	(n = 19)	(n = 13)	(n = 16)	(n = 9)	(n = 9)	(n = 11)
$V_{1/2}$ (mV)	–98.95	–91.48	–93.57	–93.22	–86.96	–86.22	–86.81	–87.37
k (mV)	6.86	6.68	6.69	6.85	5.7491	5.8	6.08	5.78

WT, wild type.

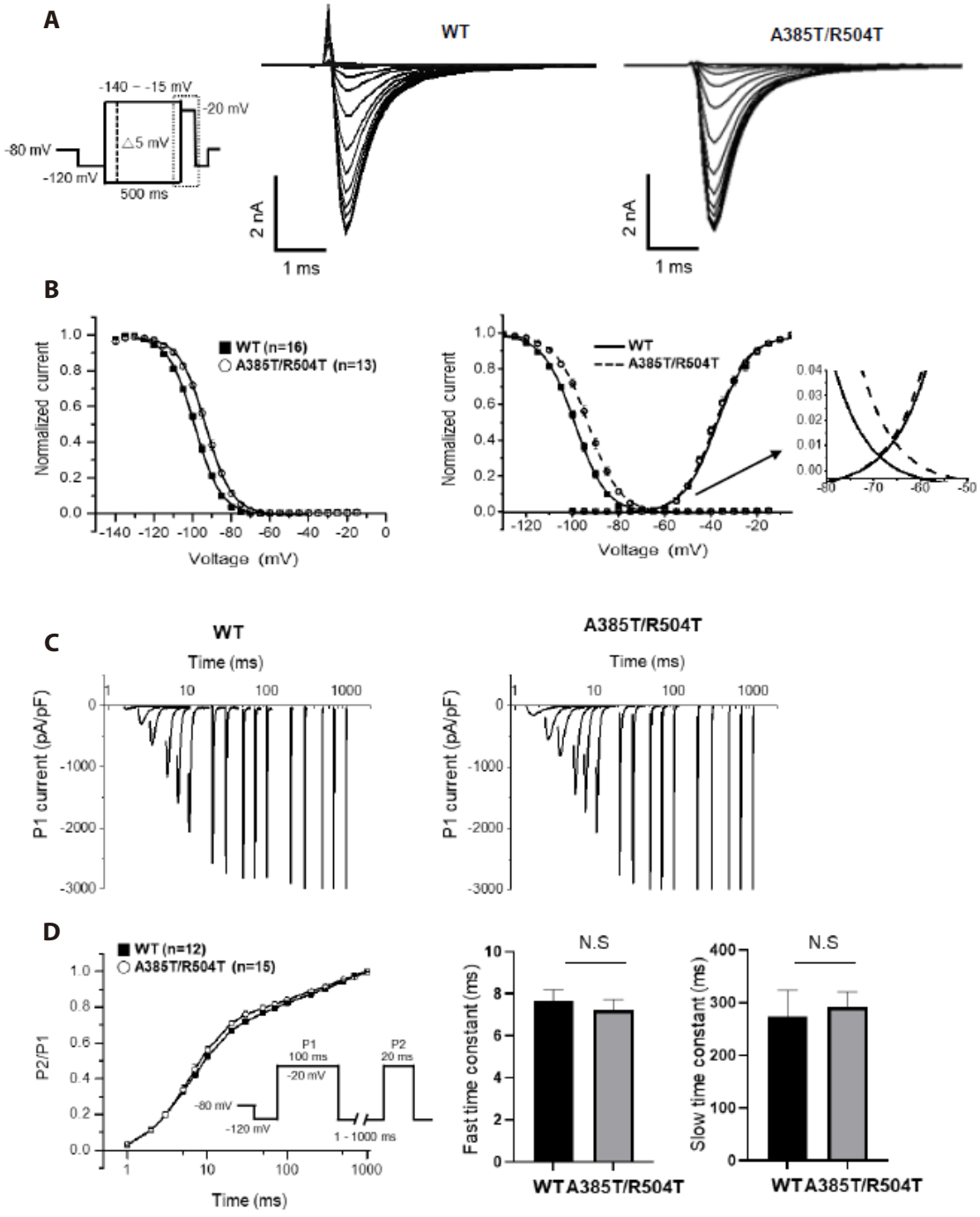

Fig. 3. Characterization of Na^+ channel property in the steady-state activation and inactivation. (A) Representative traces of voltage dependence of inactivation. The protocol is shown in left panel. (B) Voltage dependence of activation and inactivation and window current. The window current refers to the expanded segment of the overlapping region between the activation and inactivation of both the WT and p.A385T/R504T channels. (C) Time constant of recovery from inactivation to A385T/R504T was elicited with a double pulse protocol. (D) The relationship between P2/P1 and the inter-pulse interval was graphed, with curves representing double-exponential functions. The fast and slow time constants were estimated from the plotted double-exponential functions. WT, wild type; N.S, not significant.

p.R504T reducing I_{Na}, and p.A385T displaying slowed recovery.

The genes *SCN1B-SCN4B* encode the five voltage-gated sodium channel (VGSC) β subunits, with *SCN1B* encoding the β1-subunit and its splice variant, β1B, and *SCN2B-SCN4B* encoding the β2, β3, and β4 subunits, respectively [12]. The expression of VGSC β-subunits varies among tissues and cell types, including the heart, where *SCN1B* is abundantly expressing β1-subunit [13,14]. While the precise function of the interaction between *SCN5A* and *SCN1B* is unclear, it is established that modulating *SCN5A* function through *SCN1B* is important [12]. Therefore, we

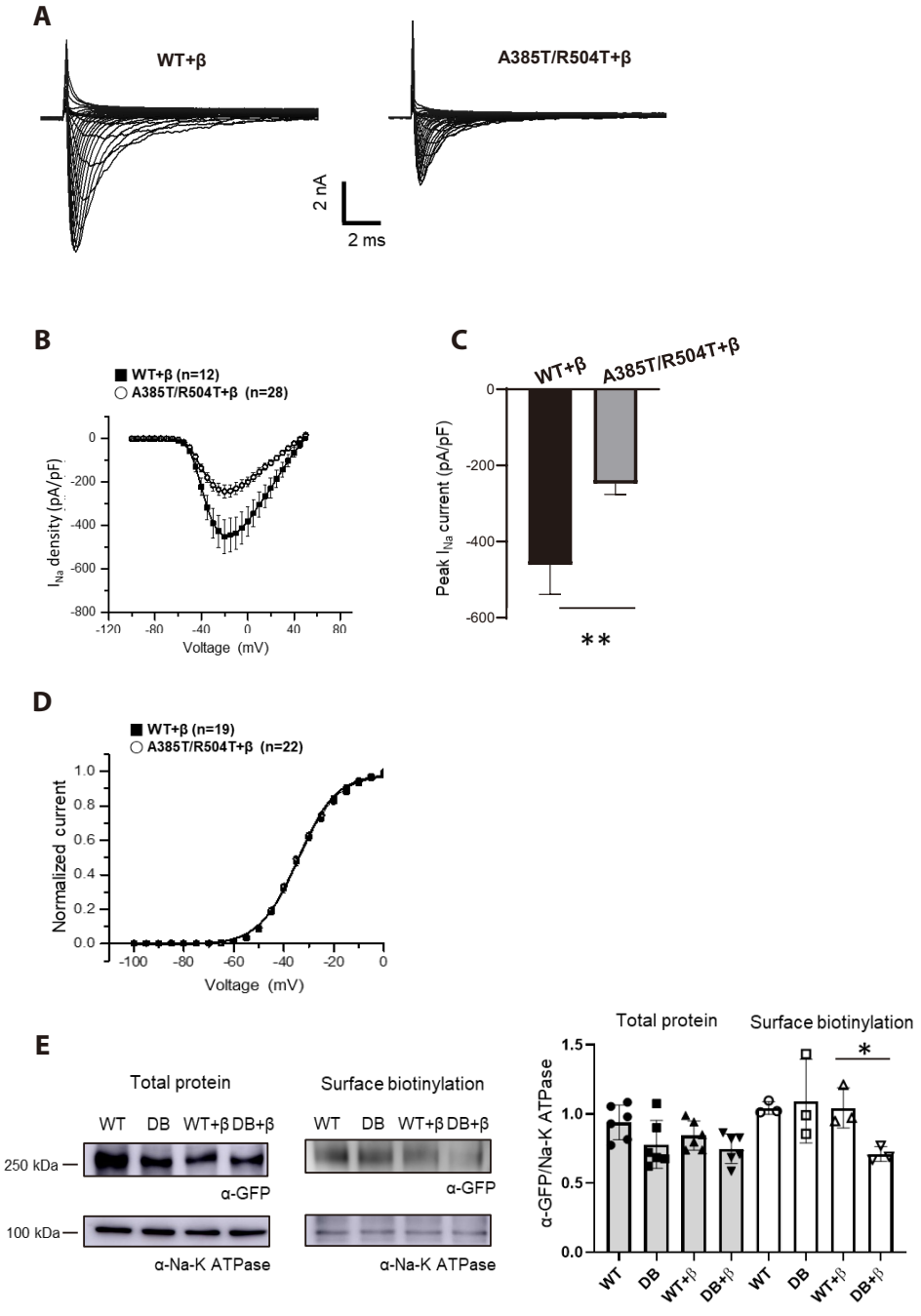

Fig. 4. Reduced p.A385T/R504T I_{Na} co-transfected with β1-subunit. (A) Representative whole-cell Na^+ current traces of WT and p.A385T/R504T in the presence of β1. (B) I-V relation of WT + β and p.A485T/R504T + β. (C) Comparison of peak I_{Na} density ($p = 0.0027$). p-value less than 0.05 was considered to be statistically significant, *$p < 0.05$; **$p < 0.01$. (D) Voltage dependence of activation for WT and p.A385T/R504T in the presence of β1-subunit measured form 12-20 cells. (E) Representative Western blotting image of $Na_V1.5$ in transfected HEK293 cells with and without β1-subunit. WT, wild type; I-V, current-voltage; DB, double mutant; GFP, green fluorescent protein.

identified the p.A385T/R504T mutant disturb interaction with *SCN1B*. Surprisingly, co-expression with β1-subunit reduced peak I_{Na} density in mutant to 48%, compared to WT (Fig. 4C). VGSC β-subunits collaborate with α-subunits to facilitate the transportation of channels to the cell membrane and modulate α-subunit activity [15,16]. Our study revealed consistent overall protein expression of *SCN5A* regardless of mutation without *SCN1B* expression. Co-expression with *SCN1B*, however, led to a significant decrease in surface protein expression, indicating likely interference of the β subunit with mutant protein trafficking. In light of diminished surface expression levels regulated by *SCN1B*, potential influences on other ion channels involved in channelosome formation were suggested [17]. For instance, Clatot *et al*. [18] recently demonstrated *SCN5A* and *KCND3* interregulation, revealing that *SCN5A* variants in BrS reduce I_{Na} and increase transient outward K^+ current (I_{to}). *KCND3* variants associated with spinocerebellar ataxia exhibit variable effects on I_{Na} based on I_{to} function. Interaction studies highlight the intricate modulation of *SCN5A* and *KCND3* channels, emphasizing the complex interplay in cardiac and neuronal syndromes [18]. Further investigations will be required to ascertain whether *SCN5A* mutations exert influences on other ion channels.

VGSC α and β subunits interact through two mechanisms: β1 and β3 noncovalently interact with α subunits *via* N and C ter-

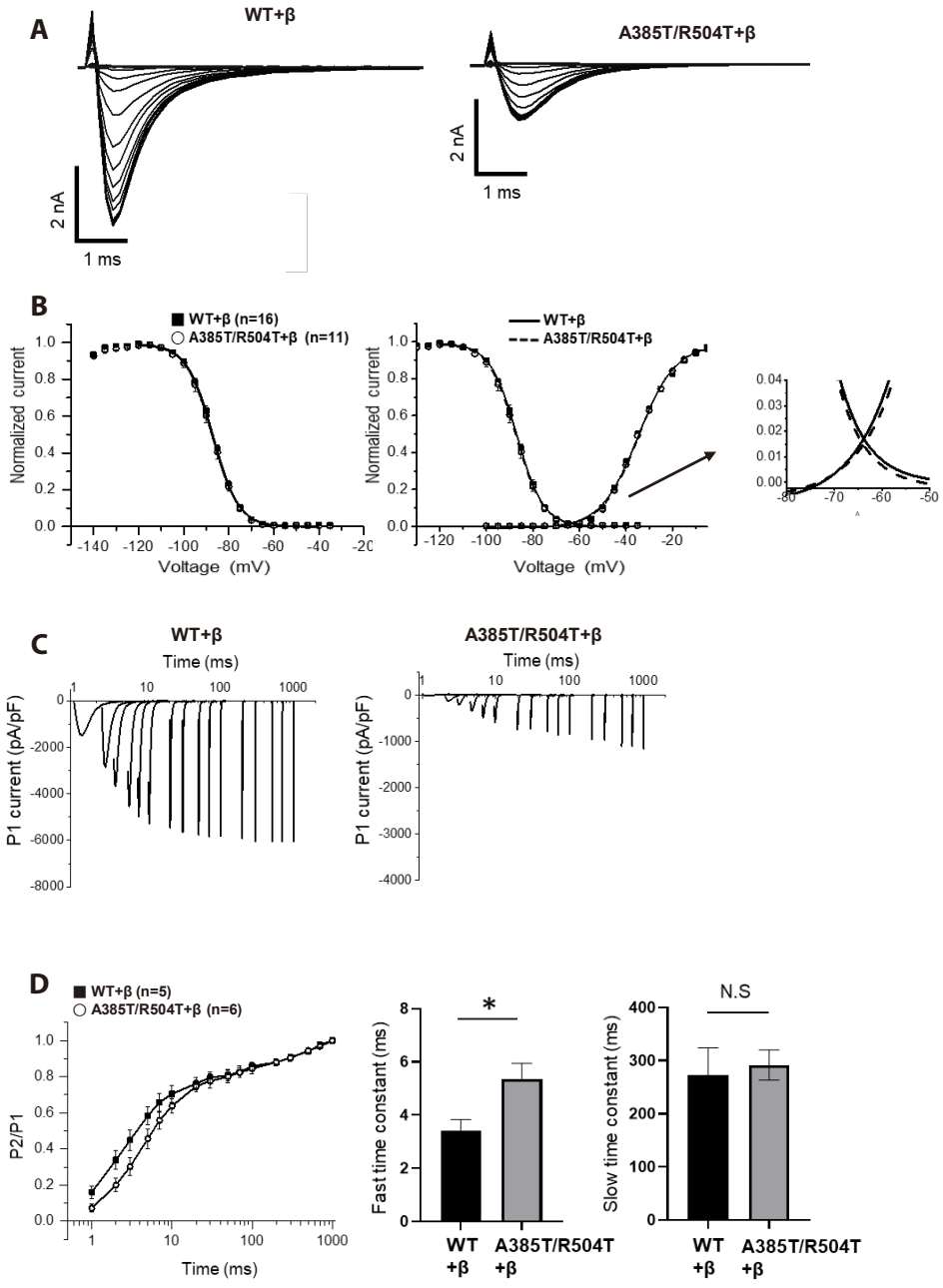

Fig. 5. Characterization of Na^+ channel property in the steady-state activation and inactivation in co-expressed β1-subunit. (A) Representative traces of voltage dependence of inactivation in the presence of β1-subunit. (B) Voltage dependence of activation and inactivation, and window current. (C) Representative traces of time course of recovery from inactivation of WT and p.A385T/R504T with β1-subunit. (D) The P2/P1 ratio was plotted against the inter-pulse interval, and the resulting curves were fitted with double-exponential functions. The time constants for the fast (p = 0.0250) and slow components were estimated from these plotted functions. p-value less than 0.05 was considered to be statistically significant, *p < 0.05. WT, wild type; N.S, not significant.

mini, while β2 and β4 form covalent interactions with α subunits through a single N-terminal cysteine [12]. In a previous study conducted by Wan *et al*. [19], co-transfection of *SCN5A* double missense mutation (p.R1232W/T1620M) with the β1-subunit resulted in a significant reduction of I_{Na} density, compared to the transfection of p.R1232W/T1620M alone. These results suggest that the p.T1620M in the extracellular S3-S4 linker in domain IV may affect its interaction with the β1-subunit, resulting in reduced stability of the α-β-subunit complex. Moreover, our findings emphasized a notable reduction in current in the presence of the p.R504T mutation when co-transfected with β1, underscoring the significance of the β1 interaction, especially with p.R504T compared to p.A385T. However, the lack of identification of specific binding sites in the α-β complex was acknowledged as a limitation in our experiments.

Slower recovery from inactivation is one of the mechanisms underlying BrS [20]. Mutations in *SCN5A* genes can result in delayed recovery from inactivation, which can lead to reduced availability of sodium channels during the cardiac action potential, causing a reduction in I_{Na} and ultimately contributing to arrhythmias such as BrS and cardiac conduction disorder [21]. In this study, similar to the β1-subunit-dependent regulation seen in the I_{Na} density reduction results (Fig. 4), the recovery of inactivation of p.A385T/R504T was slower when expressed with the β1-subunit (Fig. 5D). This suggests that the presence of β1 interaction is necessary for the reduced I_{Na} observed in a BrS patient with the novel double

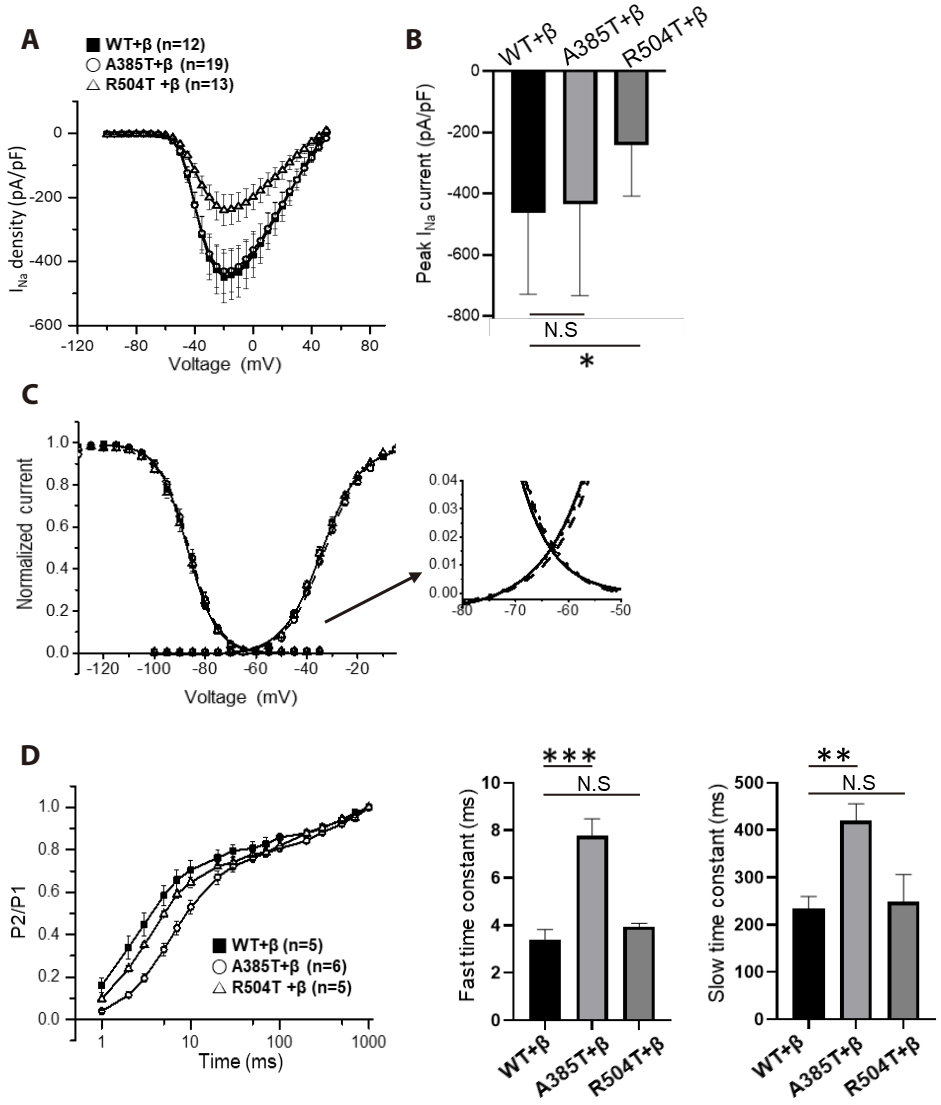

Fig. 6. Whole-cell current recordings of p.A385T and p.R504T. Na^+ channels were expressed by transfection in HEK293 cells in the presence of β1-subunit. (A) I-V relation of WT + β, p.A385T + β, and p.R504T + β. (B) Comparison of peak I_{Na} density. Compared to the WT group, p.R504T + β significantly reduced current density (p = 0.0167). *p < 0.05; **p < 0.01; ***p < 0.001. (C) Voltage dependence of activation and inactivation, and window current. (D) Time course of recovery from inactivation of WT, p.A385T, and p.R504T with β1-subunit. WT, wild type; N.S, not significant.

missense mutation (p.A385T/R504T) of *SCN5A*. When comparing recovery from inactivation for p.A385T and p.R504T, p.A385T + β1 exhibited significantly slower kinetics than WT + β1 (Fig. 6D). This result contrasts with the notable decrease in I_{Na} density observed in p.R504T + β1 (Fig. 6A). p.A385T exhibits loss-of-function characteristics in the rate of recovery from inactivation, while p.R504T displays loss-of-function properties in regulating I_{Na} density. The study's findings point to the importance of the β-subunit in modulating the effects of the p.A385T/R504T mutation on sodium channel function. These insights into the impact of specific *SCN5A* mutations and their interactions with auxiliary subunits could provide a deeper understanding of the pathophysiology of BrS. Furthermore, to understand the impact of the biophysical properties of *SCN5A* mutations on overlapping phenotypes, it would be beneficial to construct a computational cardiomyocyte-based 3D heart model for *in silico* simulation in further studies.

In conclusion, this study investigated the electrophysiological properties of novel *SCN5A* missense mutations (p.A385T/R504T). The interaction between the α-subunit *SCN5A* and β1-subunit *SCN1B* has been identified as causing loss-of-function in mutations, underscoring the potential for overlapping clinical phenotypes including BrS and CCD with LQTs. This finding also highlights the modulatory role of *SCN1B* on *SCN5A* mutations. Investigating the electrophysiological properties of these mutations could provide valuable insights into the molecular basis of and contribute to the development of more effective diagnostic and therapeutic strategies.

FUNDING

This work was supported by the National Research Foundation of Korea (NRF) funded by the Korea government (MSIT) [NRF-2018R1A5A2025964 and NRF-2021R1A2C2007 to S.J.K, NRF-2022R1A2C2009067 to H.-J.P, RS-2023-00213304 to S.W.C] and

by the Dongguk University Research Program of 2021 to S.W.C.

ACKNOWLEDGEMENTS

None.

CONFLICTS OF INTEREST

The authors declare no conflicts of interest.

REFERENCES

1. Napolitano C, Bloise R, Monteforte N, Priori SG. Sudden cardiac death and genetic ion channelopathies: long QT, Brugada, short QT, catecholaminergic polymorphic ventricular tachycardia, and idiopathic ventricular fibrillation. *Circulation*. 2012;125:2027-2034.
2. Rook MB, Evers MM, Vos MA, Bierhuizen MF. Biology of cardiac sodium channel Nav1.5 expression. *Cardiovasc Res*. 2012;93:12-23.
3. Wilde AAM, Amin AS. Clinical spectrum of SCN5A mutations: long QT syndrome, Brugada syndrome, and cardiomyopathy. *JACC Clin Electrophysiol*. 2018;4:569-579.
4. Carmeliet E. Congenital LQT syndrome from gene to torsade de pointes. *Korean J Physiol Pharmacol*. 2002;6:1-8.
5. Grant AO, Carboni MP, Neplioueva V, Starmer CF, Memmi M, Napolitano C, Priori S. Long QT syndrome, Brugada syndrome, and conduction system disease are linked to a single sodium channel mutation. *J Clin Invest*. 2002;110:1201-1209.
6. Remme CA, Wilde AA. SCN5A overlap syndromes: no end to disease complexity? *Europace*. 2008;10:1253-1255.
7. Porretta AP, Probst V, Bhuiyan ZA, Davoine E, Delinière A, Pascale P, Schlaepfer J, Superti-Furga A, Pruvot E. SCN5A overlap syndromes: an open-minded approach. *Heart Rhythm*. 2022;19:1363-1368.
8. Bezzina C, Veldkamp MW, van Den Berg MP, Postma AV, Rook MB, Viersma JW, van Langen IM, Tan-Sindhunata G, Bink-Boelkens MT, van Der Hout AH, Mannens MM, Wilde AA. A single Na(+) channel mutation causing both long-QT and Brugada syndromes. *Circ Res*. 1999;85:1206-1213.
9. Remme CA, Wilde AA, Bezzina CR. Cardiac sodium channel overlap syndromes: different faces of SCN5A mutations. *Trends Cardiovasc Med*. 2008;18:78-87.
10. Nakaya H. SCN5A mutations associated with overlap phenotype of long QT syndrome type 3 and Brugada syndrome. *Circ J*. 2014;78:1061-1062.
11. Chae H, Kim J, Lee GD, Jang W, Park J, Jekarl DW, Oh YS, Kim M, Kim Y. Considerations when using next-generation sequencing for genetic diagnosis of long-QT syndrome in the clinical testing laboratory. *Clin Chim Acta*. 2017;464:128-135.
12. O'Malley HA, Isom LL. Sodium channel β subunits: emerging targets in channelopathies. *Annu Rev Physiol*. 2015;77:481-504.
13. Gaborit N, Le Bouter S, Szuts V, Varro A, Escande D, Nattel S, Demolombe S. Regional and tissue specific transcript signatures of ion channel genes in the non-diseased human heart. *J Physiol*. 2007;582:675-693.
14. Makita N, Bennett PB Jr, George AL Jr. Voltage-gated Na+ channel beta 1 subunit mRNA expressed in adult human skeletal muscle, heart, and brain is encoded by a single gene. *J Biol Chem*. 1994;269:7571-7578.
15. Calhoun JD, Isom LL. The role of non-pore-forming β subunits in physiology and pathophysiology of voltage-gated sodium channels. *Handb Exp Pharmacol*. 2014;221:51-89.
16. Daimi H, Lozano-Velasco E, Aranega A, Franco D. Genomic and non-genomic regulatory mechanisms of the cardiac sodium channel in cardiac arrhythmias. *Int J Mol Sci*. 2022;23:1381.
17. Abriel H, Rougier JS, Jalife J. Ion channel macromolecular complexes in cardiomyocytes: roles in sudden cardiac death. *Circ Res*. 2015;116:1971-1988.
18. Clatot J, Neyroud N, Cox R, Souil C, Huang J, Guicheney P, Antzelevitch C. Inter-regulation of K_v4.3 and voltage-gated sodium channels underlies predisposition to cardiac and neuronal channelopathies. *Int J Mol Sci*. 2020;21:5057.
19. Wan X, Wang Q, Kirsch GE. Functional suppression of sodium channels by beta(1)-subunits as a molecular mechanism of idiopathic ventricular fibrillation. *J Mol Cell Cardiol*. 2000;32:1873-1884.
20. Zimmer T, Surber R. SCN5A channelopathies--an update on mutations and mechanisms. *Prog Biophys Mol Biol*. 2008;98:120-136.
21. Han D, Tan H, Sun C, Li G. Dysfunctional Nav1.5 channels due to SCN5A mutations. *Exp Biol Med (Maywood)*. 2018;243:852-863.